Bulgarian Journal of Physics **28** Nos 5/6 (2001) 225–237

A SIMPLE METHOD FOR DETERMINING THERMAL CONDUCTIVITY COEFFICIENTS OF CONDUCTING THIN FILMS

CHI HSIANG PAN
Department of Mechanical Engineering
National Chin-Yi Institute of Technology
Taichung, Taiwan

Abstract. We present a simple method to determine thermal conductivity coefficients (TCC) of conducting thin films using a compact micromachined test structure and common experimental apparatus. The test structure is fabricated by a sacrificial-layer surface micromachining technique with one mask process, and the measurements are performed using an optical microscope together with probe stages, a power supply and a heating stage, which are available in a laboratory. Analytical expressions are derived to calculate the thermal conductivity coefficients of thin films from the experimental data. Instead of conventional electrical methods that apply Joule-heating to the rising of a temperature gradient at a test structure and use polysilicon resistors as thermometer to monitor the temperature, our work proposes a temperature-displacement method to determine the temperature of test structure. Experimental results with a phosphorous-doped LPCVD polycrystalline silicon film are used to demonstrate the effectiveness of the proposed method. The obtained thermal conductivity coefficients show a small decrease as temperature increases, and its average value is around 39 $\mathrm{W\,m^{-1}\,{}^{\circ}C^{-1}}$ in the temperature range from room temperature to 400 °C.

PACS number: 68.90.+g

1. Introduction

Thermal conductivity coefficients (TCC) of thin film materials are vital for the design and performance of thermal microsensors, thermal MEMS devices, integrated circuits, and electronic packages [1–6]. There are well-documented thermal conductivity data of bulk materials, but they may not be directly appli-

© 2003 St. Kliment Ohridski University Press All rights reserved

cable to thin films with various thicknesses and process-dependent properties [7-13]. The discrepancies between thin films and bulk data indicate the importance of determining TCC of thin films. Presently, several noticeable methods that utilize such simple micromachined test structures as bridges, beams and membranes for determining TCC of thin films have been developed [11-17]. For example, the method in [13] uses suspended membranes as test structures that are fabricated by deep reactive ion etching of single-crystal Si with a deposited SiO_2 layer as the etch stop. Electrical resistance thermometry and Joule-heating in the aluminum bridges are utilized in this work to measure and predict the influence of impurity type and concentration on the TCC of polysilicon films at temperatures between 20 K and 320 K. Methods in [14-17] apply microcantilevers to be test structures which are fabricated with a commercial CMOS process and post-processed by anisotropic bulk etching. These methods use a polysilicon resistor as a Joule-heating power to establish a temperature gradient at the tip location of test structure and use other polysilicon resistors located at different locations as resistance thermometers to measure the temperature. According to the operating principle, two test structures are required to determine the TCC of thin film. One test structure is used as a reference, and the other is a modified structure for the characterization of measured film. Therefore, the TCC of measured film is determined in comparison with the reference. Taking a review of the above methods, it is found that they require expensive experimental apparatus and sophisticated preparation of specimens. Besides, the temperature range of interest in measuring TCC is at lower temperature of the commercial IC's operating range 20 K to 400 K, for example. However, the characterization of TCC over an extended temperature range, especially at high temperature is becoming emergent for thermal MEMS devices. Therefore, a simple and convenient method for determining TCC of thin films is highly desirable.

In this paper, we present a simple method to determine TCC of single-layer conducting thin films using a compact test structure and common experimental apparatus. The test structure is fabricated by sacrificial-layer surface micromachining techniques with one mask process, and the measurements are performed using an optical microscope along with probe stages, a power supply and a heating stage, which are available in a laboratory. Analytical expressions are derived to calculate the TCC of thin films from the experimental data. Instead of conventional electrical methods that apply Joule-heating to the rising of a temperature gradient at a test structure and use polysilicon resistors as thermometer to monitor the temperature, we propose a temperature-displacement method to determine the temperature of test structure. Since doped polycrystalline silicon films are widely used in a variety of IC and MEMS applications, experimental results with phosphorous-doped LPCVD polysilicon films

are used to demonstrate the effectiveness of the proposed method.

2. Operating Principle

Figure 1 schematically depicts the test structure in our study, which is similar to those in [18, 19]. The test structure consists of a pair of cantilever beams with different lengths connected by a short tip beam. The beams are made of the measured conducting film. Two cantilever beams are designed as test beams and the tip beam acts as an indicator. By applying current through the beams, a temperature rise throughout the test structure causes the deflection of the beams, which is resulted from the difference of elongation of the two cantilever beams. Therefore, a displacement is generated at a free end of the tip beam. A Vernier gauge located at free end of the indicator beam can be used to quantify the displacement, but this is optional. Since the displacement of the tip beam is sufficiently large, direct observations under a microscope mounted with a ruler or a CCD camera can be made to collect reasonably accurate data. Analytical expressions are derived to relate the displacement to the TCC of the measured film.

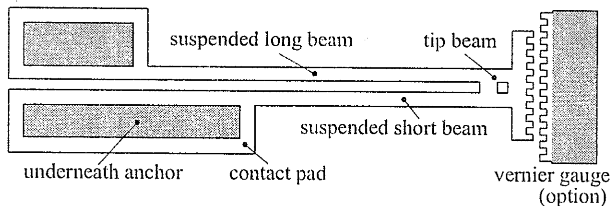

Fig. 1. The schematic diagram of test structure (top view)

3. Analytical Expressions

3.1. Electro-thermal Relationship

Figure 2 shows the electro-thermal model of test structure. l_1 and l_2 represent the lengths of long test beam and short test beam, respectively. w and h denote the width and thickness of beams, respectively. A rigid beam connects the free ends of two cantilever beams. s denotes the distance (or gap) between centerlines of the two beams ($s \ll l_1, l_2$). Symbol K denotes the thermal conductivity coefficient, ρ is the electrical resistivity of the film, and J denotes the current density through the beams. By feasible assumption, the heat losses by conduction to the air, by free convection, and by radiation can be neglected as compared to the heat loss by conduction through the test structure to the contact pads (heat sinks) under low temperature and in high vacuum [6, 11, 20, 21]. Therefore, the heat flow Q in longitudinal direction of the beams is much

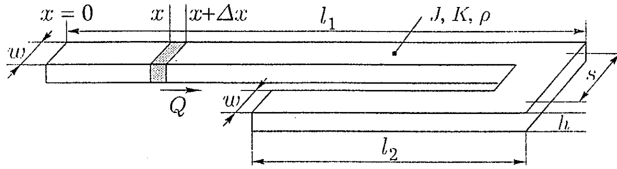

Fig. 2. The electro-thermal model of test structure

more than that in lateral directions. Furthermore, since the two cantilever beams are much longer than the tip beam, and the beam size in the length direction is much larger than that of its cross-section, one dimension model of heat equation is used to find the electro-thermal relationship between electrical power and temperature along the beams. According to the heat transfer under steady-state condition, the second-order differential equation is obtained

$$K\frac{\mathrm{d}^2T(x)}{\mathrm{d}x} = -J^2\rho(T(x)) \tag{1}$$

where $T(x)$ is the temperature profile along the beams, and $\rho(T(x))$ is the temperature dependent electrical resistivity with a linear temperature coefficient ε, such that

$$\rho(T(x)) = \rho_0(1 + \varepsilon(T(x) - T_0)\,. \tag{2}$$

ρ_0 denotes the electrical resistivity at room temperature T_0. From Eqs (1) and (2), and the boundary conditions $T(0) = T_p$ and $T(l) = T_p$, the temperature profile can be solved as [6]

$$T(x) = \frac{\left(T_p - T_0 + \frac{1}{\varepsilon}\right)(\cos(\lambda x) + (1 - \cos(\lambda l)))}{\sin(\lambda l)\sin(\lambda x) + T_0 - \frac{1}{\varepsilon}} \tag{3}$$

T_p denotes the contact pad temperature and is assumed to be T_0, $l = l_1 + l_2 + s$, and

$$\lambda = \sqrt{\frac{J^2\rho_0\varepsilon}{K}}\,. \tag{4}$$

The average temperature change ΔT along the test structure is defined as

$$\Delta T = \frac{1}{l}\int_0^l T(x)\,\mathrm{d}x - T_0\,. \tag{5}$$

Therefore, the thermal conductivity coefficient K can be obtained from Eq. (5) together with Eq. (3) and Eq. (4), if the temperature change ΔT is determined

beforehand and all other parameters such as ρ_0, ε and J are either known or measurable.

3.2. Thermal-Mechanical Relationship

Figure 3 depicts the thermal-mechanical model of test structure. When temperature rises, the difference between the two cantilever beams with respect to elongation is denoted by ∇. Meanwhile, a reactive bending moment M, an axial force P, and a transverse force F are induced at the boundary, as shown in Fig. 3(b). Therefore, the system can be considered as two connected beams subjected to a bending moment, an axial force, and a transverse force at the fixed end of long test beam to have the difference of the elongation ∇, as shown in Fig. 3(c).

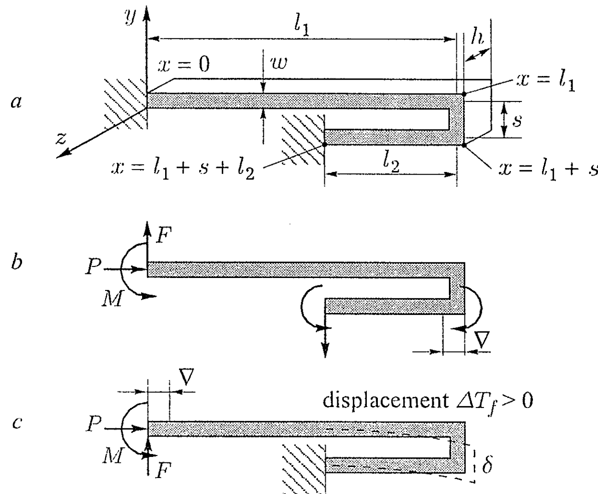

Fig. 3. The thermal-mechanical model of test structure

Thus

$$\nabla = l_1\xi_1 - l_2\xi_2\,. \tag{6}$$

The axial strain ξ_1 in the long beam is found as $\xi_1 = \alpha\Delta T - \dfrac{P}{EA_b}$, and the axial strain ξ_2 in the short beam is $\xi_2 = \alpha\Delta T + \dfrac{P}{EA_b}$, respectively. Symbol α denotes the thermal expansion coefficient, E is the Young's modulus, and A_b is the cross section area of beams. α and E are either known or measurable and assumed constant here. Thus

$$\nabla = \alpha\Delta T(l_1 - l_2) - (l_1 + l_2)\frac{P}{EA_b}\,. \tag{7}$$

By unit-load method [22] in calculating displacements from Eq. 7, displacement δ can be expressed as a function of the temperature change ΔT

$$\delta = \alpha\gamma\Delta T\,. \tag{8}$$

Thus, the temperature change ΔT can be derived as

$$\Delta T = \frac{\delta}{\alpha\gamma}\,. \tag{9}$$

γ is a conversion factor and is related to geometrical parameters of the test structure, including l_1, l_2, s and w only

$$\gamma = \frac{2\begin{vmatrix} a_1 & b_1 & c_1 \\ a_2 & b_2 & c_2 \\ a_3 & b_3 & c_3 \end{vmatrix}}{l_1 l_2^2\left[S\begin{vmatrix} b_2 & c_2 \\ b_3 & c_3 \end{vmatrix} - \left(l_1 - \frac{2}{3}l_2\right)\begin{vmatrix} a_2 & c_2 \\ a_3 & c_3 \end{vmatrix} + \begin{vmatrix} a_2 & b_2 \\ a_3 & b_3 \end{vmatrix}\right]} \tag{10}$$

The formulas for the coefficients in Eq. (10) are listed in Table 1.

Table 1. The formulas for the coefficients in Eq. (10)

$a_1 = (l_1 + l_2)I/A_b + \frac{1}{3}s^3 + s^2 l_2$ $= \frac{1}{12}(l_1 + l_2)w^2 + \frac{1}{3}s^3 + s^2 l_2$ $(I = \frac{1}{12}hw^3,\quad A_b = hw)$	$b_1 = \frac{1}{2}s^2 l_1 + s l_1 l_2 - \frac{1}{2}s l_2^2$	$c_1 = \frac{1}{2}s^2 + s l_2$
$a_2 = \frac{1}{2}s^2 l_1 + s l_1 l_2 - \frac{1}{2}s l_2^2$	$b_2 = \frac{1}{3}l_1^3 + l_2 l_1^2$ $- l_1 l_2^2 + \frac{1}{3}l_2^3 + s l_1^2$	$c_2 = \frac{1}{2}l_1^2 + l_1 l_2$ $- \frac{1}{2}l_2^2 + s l_1$
$a_3 = \frac{1}{2}s_2 + s l_2$	$b_3 = \frac{1}{2}l_1^2 + l_1 l_2$ $- \frac{1}{2}l_2^2 + s l_1$	$c_3 = l_1 + l_2 + s$

4. Test Structures Fabrication

The test structures employed in measurement are made of LPCVD polycrystalline silicon films at 620 °C with a silane (SiH_4) flow rate of 40 sccm and deposition time of 260 min, following a high temperature phosphorus-diffusion step (POCL3) at 900 °C deposition about 40 minutes and with 1050 °C drive-in and annealing for 1 hour. The film thickness is about 2 μm. PECVD TEOS SiO_2 with about thickness of 3 μm is used as a sacrificial layer. Finally, the test structures are fabricated by a conventional surface-sacrificial layer micromachining technique, as shown in Fig. 4.

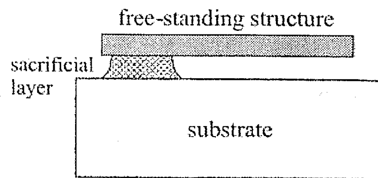

Fig. 4. The basic surface-sacrificial micromachining process for free-standing test structures

5. Experiments and Discussions

5.1. Experiments

Figure 5 shows the experimental apparatus. It consists of an optical microscope mounted with a CCD and two devices placed under the microscope. The CCD is connected to the computer with installed imaging software (Matrox Inspector version 3.1) for image capture, measuring, analysis and processing. The two devices: one is a temperature-controlled heating stage, and the other is a pair of probe stages are connected with a current/voltage adjustable power supply.

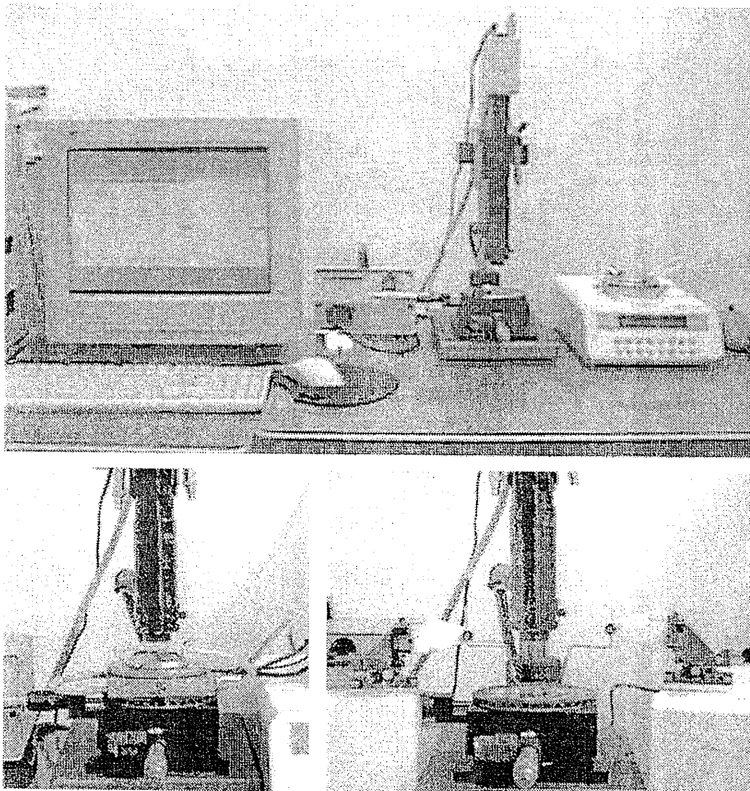

Fig. 5. Experimental apparatus

According to Eqs (3) to (5) and Eq. (9), it is found that the current density J, the electrical resistivity ρ_0, the temperature coefficient of resistivity ε and the thermal expansion coefficient α of test structure must be obtained before determining the thermal conductivity coefficient K.

Experimental procedures carried out to determine the parameters are described below. In the first step, the heating stage is placed under the microscope to heat up the test structure, and the relationship between displacement δ and temperature change ΔT can be obtained. Therefore, according to Eq. (8), the thermal expansion coefficient α of around 2.7×10^{-6} is obtained in the temperature range from room temperature to 400 °C. The detailed knowledge of obtaining the thermal expansion coefficient is in Ref. [19]. In order to prevent either creep or recrystallization, measurements are made on each sample in the temperature range from room temperature to 400 °C. In the second step, probe stages connected with a power supply are placed under the microscope to apply current/voltage dissipating a heating power through the test structure.

Applying current I to the test structure and measuring displacement δ, the displacement-current (δ-I) relationship is obtained. After that, we relate the δ-I relationship to the displacement-temperature (δ-T) relationship, which is derived from Eq. (8). Then the I-T diagram is obtained, as shown in Fig. 6.

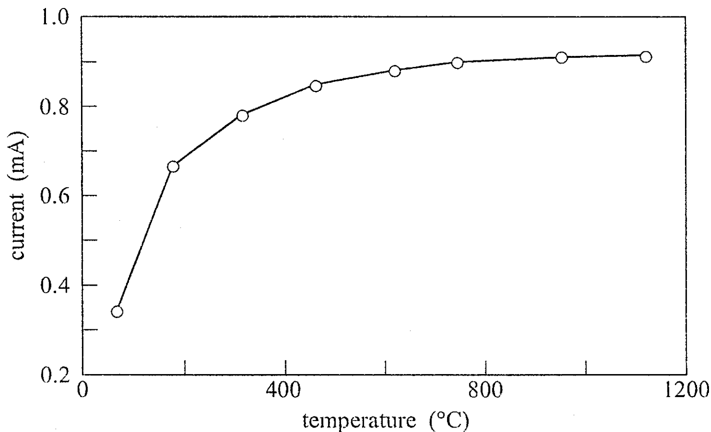

Fig. 6. Current-temperature (I-T) diagram

Different voltages V are applied to the test structures, meanwhile the displacements δ are measured. Therefore, the displacement-voltage (δ-V) relationship and the current-voltage (I-V) relationship (Fig. 7) are obtained simultaneously. After that, relating the δ-V relationship to the displacement-temperature (δ-T) relationship, which is derived previously, thus the V-T relationship is obtained.

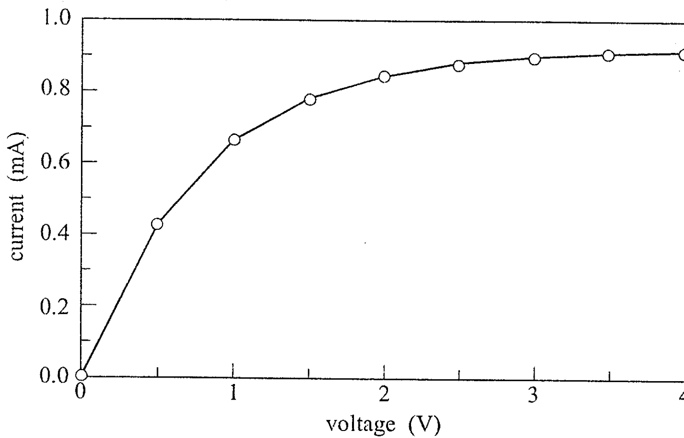

Fig. 7. Current-voltage (I-V) diagram

According to the I-V relationship and the Ohmic principle $R = V/I$, the resistance-voltage (R-V) relationship is obtained. R denotes the total resistance of the measured system. Subsequently, relating the R-V relationship with the V-T relationship, thus the R-T relationship is obtained. Since the total resistance R is composed of the resistance of test structure and the contact resistance, it is required to know the contact resistance beforehand for determining the resistivity of thin film accurately. The value of contact resistance can be obtained by plotting the total resistances of test structures with different beam lengths and by extracting the intercept resistance corresponding to the length of zero, which is the contact resistance. Subsequently, subtracting the contact resistance from the total resistance, the resistivity-temperature characteristics of test structure is obtained, as shown in Fig. 8. Using Eq. (2) to fit the characteristics linearly with ε as the only fitting parameter and calculating the slope of the line, thereby ε is obtained. From some sets of measurements, ε is about 2.3×10^{-3} $^{\circ}\mathrm{C}^{-1}$. By the way, the value of ρ_0 can also be obtained and is around 2.5×10^{-5} $\Omega\,\mathrm{m}$. The current density J is calculated by $J = I/A_b$.

Since the parameters α, J, ρ_0 and ε are known, the thermal conductivity coefficient K is calculated from Eqs (3) to (5) with K as only one unknown parameter. The calculated values of TCC of phosphorous-doped polysilicon thin film are under a deviation of 0.25 $\mathrm{W\,m^{-1}\,^{\circ}C^{-1}}$. It is found that the thermal conductivity coefficients are reduced a little as temperature increases. The average value is around 39 $\mathrm{W\,m^{-1}\,^{\circ}C^{-1}}$ in the temperature range from room temperature to 400 °C. More recently, the thermal conductivity of doped polysilicon films has been reported to 14-42 $\mathrm{W\,m^{-1}\,^{\circ}C^{-1}}$ [11-17]. The difference in the values often results from process conditions, impurity concentrations and

grain size of thin films. From this viewpoint, it indicates that a convenient and accurate method for determining TCC of thin films is highly desirable. Figures 9 and 10 show the photographs of test structures at an initial state and operating state, respectively. Figure 10 is a symmetric design, in which two independent test structures are constructed symmetrically in the test sample. In this manner, the double displacement can be obtained by taking the difference of the distance between two tip beams.

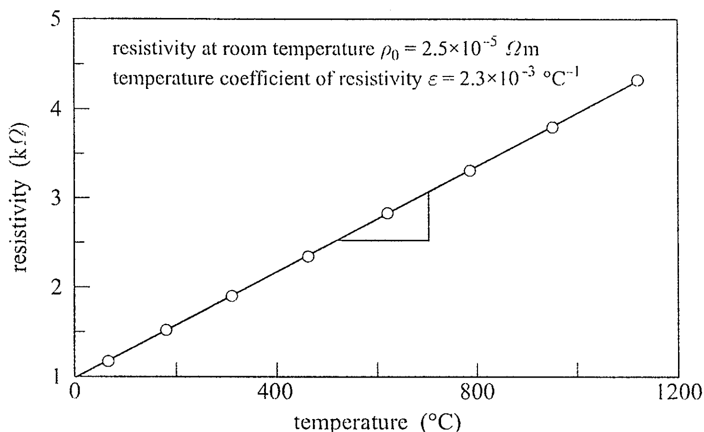

Fig. 8. Resistance-temperature (R-T) diagram for determining the temperature coefficient of resistivity ε

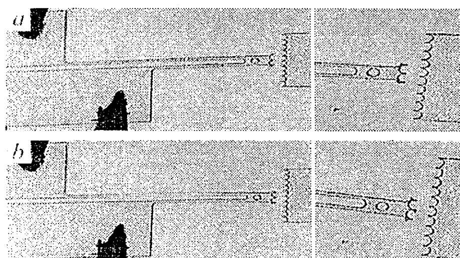

Fig. 9. Photographs of a test structure: (a) initial state, (b) operating state

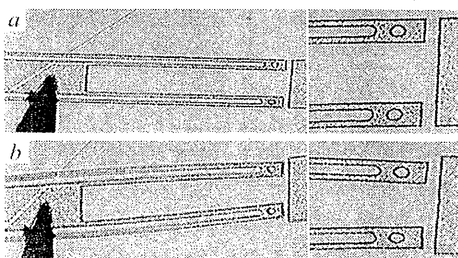

Fig. 10. Photographs of a test structure with symmetric design: (a) initial state, (b) operating state

5.2. Discussions

Compared to conventional methods, there are some merits in our method: (1) the test structure is quiet compact and easily fabricated, and the experimental apparatus is available in the laboratory; (2) the temperature of Joule-heated test structure is determined by measuring the displacement of the test structure, and the displacement can be directly measured under an optical microscope

equipped with a ruler or a CCD camera to collect reasonable accurate data; (3) the resistivity-temperature characteristic of thin films is obtained without using any semiconductor parameter analyzer, such as 4145B HP; (4) no thermal contact resistance at the interface between any other layers is under consideration. Except merits, some potential factors that influence the uncertainty of results are considered. The first factor is dominated by the side walls of test beams free from vertical. This is resulted from the isotropic etching of beams in our experiment. However, the effect can be less than 1.5 %. The detailed knowledge of the influence of cross section geometry is in reference [18]. The solvable method to reduce the effect is to use anisotropic-RIE (Ion Reactive Etching) to produce vertical side walls. The second factor is the undercut of anchor beneath the contact pads, which is due to the isotropic etching of sacrificial layer. This makes the boundary condition of anchors slightly different from ideal geometry. Fortunately, this factor makes little deviation in the displacement of test structure. The third and fourth factors are dominated by contribution from the pad resistance and the various contact resistances of probes at pads, respectively. These will influence the thermal response and the I-V characteristics of test structure. However, for long test beams and large pads, the pad resistance is much smaller than the resistance of test beams, so the temperature at pad supports can be assumed essentially near the ambient temperature [6, 11, 20] and the deviation of the thermal response of test structure can be neglected. As for the varying contact resistance between the probes and the pads, it can be reduced using aluminum metallization pads or bonding with wires. The fifth factor is that there is a degree of uncertainty in the predicted heat losses from the test structure through the heat convection and radiation conditions. This can be studied in detail further. The initial position of the tip beam of the test structure would be moved from its designed position due to the residual strain of thin film, but this makes no problem in measurement because we need only the difference of the tip site.

6. Conclusions

This work presents a simple method for determining thermal conductivity coefficients of conducting thin films based on the behavior of test structures produced with the films. Compared to the previous reported methods, the method possesses some advantages:

1. The proposed test structures are quiet compact and easily fabricated, and no thermal contact resistance at the interface between any other layers is under consideration;
2. The experimental apparatus is available in a laboratory;

3. The temperature of Joule-heated test structure is obtained by measuring the displacement of the test structure, and the displacement can be directly measured under an optical microscope equipped with a ruler or a CCD camera to collect reasonable accurate data;
4. The resistivity-temperature characteristic of the test structure is obtained without using any semiconductor parameter analyzer.

Experimental results with a phosphorous-doped LPCVD polycrystalline silicon film are used to demonstrate the effectiveness of the proposed method. The obtained thermal conductivity coefficient is reduced a little as temperature increases, and the average is around $39\ \mathrm{W\,m^{-1}\,{}^{\circ}C^{-1}}$ in the temperature range from room temperature to 400 °C. Modifying the test structure and analytical model to measure thermal conductivity coefficients of dielectric thin films have been studied in [23].

Acknowledgements

This work is supported by the National Science Council of the Republic of China under Contract No NSC 90-2212-E-167-002. The staffs of the Semiconductor Research Center at National Chiao Tung University are also appreciated, along with Dr W. Hsu for providing graduate students.

References

1. H. Baltes, O. Paul and O. Brand. *Micromachined, Thermally-based CMOS Microsensors*. Proc. IEEE **86** (1998) 1660-1678.
2. Y. Lee, S. Murarka, S.-P. Teng and B. Auman. *Investigation of the Low Dielectric Constant Fluorinated Polyimide for Use as the Interlayer Dielectric in ULSI*. In: Proc. Materials Res. Soc. Symp. **381** (1995) 31-43.
3. J. Suh, S. Glander, R. Darling, C. Storment and G. Kovacs. *Organic Thermal and Electrostatic Ciliary Microactuator Array for Object Manipulation*. Sensors and Actuators A **58** (1997) 51-60.
4. A. Sauter and W. Nix. *Finite Element Calculations of Thermal Stresses in Passivated and Unpassivated Lines Bonded to Substrates* . In: Proc. Mater. Res. Soc. Symp. **188** (1990) 15-20.
5. J. Orchard-Webb. *Thermal Resistance of Packages*, Engineering Report, Plessey Semiconductors (1970).
6. G. Fedder and R. Howe. *Thermal Assembly of Polysilicon Microstructures*. In: Proc. Micro Electro Mechanical Systems (Nara 1991) 63-68.
7. K. Bean, H. Hentzschei and D. Colman. *Thermal and Electrical Anisotropy of Polycrystalline Silicon*. J. Appl. Phys. **40** (1969) 2358-2359.
8. J. Lambropoulos, S. Jacobs, S. Burns, L. Shaw-Klein and S. Hwang. *Thermal Conductivity of Thin Films Measurement and Microstructural Effects*. ASME Heat Transfer Divion (Dec. 1-6, 1991) 21-32.

9. K. Goodson, M. Flik, L. Su and D. Antoniadis. *Annealing-temperature Dependence of the Thermal Conductivity of LPCVD Silicon-dioxide Layers*. IEEE Electron Device Lett. **14** (1993) 490-492.
10. H. Schafft, J. Suehle and P. Mirel. *Thermal Conductivity Measurements of Thin-film Silicon Dioxide*. In: Proc. IEEE ICMITS (1989) 121-125.
11. Y. Tai, C. Mastrangelo and R. Muller. *Thermal Conductivity of Heavily Doped Low-Pressure Chemical Vapor Deposited Polycrystalline Silicon Films*. J. Appl. Phys. **63**(5) 1 (1988) 1441-1447.
12. C. Mastrangelo and R. Muller. *Thermal Diffusivity of Heavily Doped Low Pressure Chemical Vapor Deposited Polycrystalline Silicon Films*. Sensors and Materials **3** (1988) 133-142.
13. A. McConnell, S. Uma and K. Goodson. *Thermal Conductivity of Doped Polysilicon Layers*. J. Microelectromechanical Systems **10**(3) (2001) 360-369.
14. V. Martin, O. Paul and H. Baltes. *Process-dependent Thin-film Thermal Conductivities for Thermal CMOS MEMS*. J. Microelectromechanical Systems **19**(1) (2000) 136-145.
15. F. Volklein and H. Baltes. *A Microstructure for Measurement of Thermal Conductivity of Polysilicon Thin Films*. J. Microelectromechanical Systems **1**(4) (1992) 193-196.
16. O. Paul and H. Baltes. *Thremal Conductivity of CMOS Materials for the Optimization of Microsensors*. J. Micromech. Microeng. **3** (1993) 110-112.
17. O. Paul, J. Korvink and H. Baltes. *Determination of the Thermal Conductivity of CMOS IC Polysilicon*. Sensors and Actuators A **41-42** (1994) 161-164.
18. C. Pan and W. Hsu. *A Microstructure for in-situ Determination of Residual Strain*, IEEE J. Microelectromechanical Systems **8**(2) (1999) 200-207.
19. C. Pan. *A Simple Method for Determining Linear Thermal Expansion Coefficients of Thin Films*, J. Micromech. and Microeng. **12** (2002) 1-8.
20. L. Lin and M. Chiao. *Electrothermal Responses of Line Shape Microstructures*. Sensors and Actuators A **55** (1996) 31-41.
21. R. Jones and S. Wesolowski. *Electrical, Thermoelectric, and Optical Properties of Strongly Degenerate Polycrystalline Silicon Films*, J. App. Phys. **56** (1984) 1701-1706.
22. S. Timoshenko and J. Gere. *Mechanics of Materials*. PWS Publishing Company, 3rd edn, 1990, pp 632-647.
23. C. Pan and C. Tung. *A Simple Method for Determination of Thermal Conductivity Coefficients of Dielectric Films*. In: Int. Symposium on Micromechatronics and Human Science, Nagoya, Japan, Sept. 2001, pp 10-12.
24. Q.-A. Huang and N. Lee. *Analysis and Design of Polysilicon Thermal Flexure Actuator*. J. Micromech. Microeng. **9** (1999) 64-70.